Dynamic Buffer Size Allocation in Wireless Mesh Networks for Non-Elastic Traffic

Rumipamba Zambrano R.*; Vázquez-Rodas A.; de la Cruz Llopis L.J.***;Sanvicente Gargallo E.******

**Corporación Nacional de Telecomunicaciones, Quito, Ecuador*
e-mail: ruben.rumipamba@cnt.gob.ec; rdrz83@gmail.com
*** UniversitatPolitècnica de Catalunya, Barcelona, España*
e-mail: andres.vazquez@entel.upc.edu
*** *UniversitatPolitècnica de Catalunya, Barcelona, España*
e-mail: luis.delacruz@entel.upc.edu
*** **UniversitatPolitècnica de Catalunya, Barcelona, España*
e-mail: e.sanvicente@entel.upc.edu

Resumen: Parámetros fundamentales del desempeño de las redes de comunicaciones tales como la probabilidad de pérdida de paquetes, el retardo de extremo a extremo, la utilización de los canales de transmisión, etc., se ven altamente influenciados por el tamaño de los buffers de los equipos de red. Estos parámetros afectan directamente la calidad del servicio percibida por los usuarios finales. Un dimensionamiento dinámico del tamaño de los buffers, a más de favorecer una asignación óptima de memoria, ayuda a prevenir retardos exagerados y otros problemas asociados a buffers excesivamente grandes. Sin embargo, determinar dinámicamente el tamaño de buffer adecuado que cumpla con algún requisito específico de calidad de servicio, como la probabilidad de pérdida, requiere el conocimiento exacto de ciertas funciones de distribución de probabilidad que en la práctica rara vez se encuentran disponibles. Una posible alternativa a este problema consiste en hacer que los dispositivos de red midan ciertos parámetros disponibles y a partir de ellos inferir la información restante mediante la aplicación del principio de máxima entropía. Por otra parte, los dispositivos inalámbricos imponen restricciones adicionales debido al uso de canales compartidos y más aún el efecto multi-salto en redes inalámbricas de malla sin infraestructura. Éste artículo se centra en la implementación y evaluación de un mecanismo de dimensionamiento dinámico de buffers basado en máxima entropía en redes inalámbricas de malla. Los resultados obtenidos verifican el correcto funcionamiento y la mejora de prestaciones en diversos escenarios.

Palabras clave: Dimensionamiento de buffers, redes inalámbricas de malla, pérdida de paquetes, máxima entropía, sistemas de colas.

Abstract: Fundamental network performance parameters as the packet loss probability, end-to-end delay, utilization of transmission channels, etc., are highly influenced by the buffer size of network devices. These parameters directly affect the quality of service perceived by end users. A dynamic buffer sizing can provide optimal memory allocation, and also helps to prevent exaggerated delays and other problems associated with excessively large buffers. Nevertheless, a dynamic determination of the proper buffer size that meets any specific quality of service requirement, as the packet loss probability, needs the exact knowledge of certain probability distribution functions which in practice are rarely available. A possible alternative to this problem is that network devices measure some available parameters and from them infer the remaining information by applying the maximum entropy principle. On the other hand, wireless devices impose additional restrictions due to the use of shared channels and even more to the multi-hop effect in infrastructure-less wireless mesh networks. This article focuses on the implementation and evaluation of a dynamic buffer sizing mechanism based on maximum entropy when it is applied in wireless mesh networks. Simulation results verify the proper operation and improved performance in different mesh scenarios.

Keywords: Buffer sizing, wireless mesh networks, packet loss, maximum entropy, queuing systems.

1. INTRODUCCION

For telecom operators it is very important to offer data transmissions with Quality of Service (QoS), especially when sensible and critical data are sent through the network. The typical parameters to guarantee are: bandwidth, packet loss, end-to-end delay, and delay jitter. The required QoS level is guaranteed by a proper allocation of the available resources. Common network resources are the bandwidth and the amount of memory for buffering. This work focuses on the memory resources intended for buffering.

With the increasing popularity of multimedia and real time applications, service differentiation has become more important. In this case, services are distributed in different

packet queues, each of them with a specific priority. Obviously, the more sensible data (e.g. network control messages) are assigned to the highest priority queue. After those, intermediate queues are for real time applications like voice or video. Finally, applications without QoS requirements will be allocated in the queue with the lowest priority.

In this context, it is a very common practice that each independent queue has been assigned with a fixed specific size. The reduction of memory costs joint with the aim of preventing packet losses has motivated the spread of huge buffers over most of the network devices. This problem, currently known as *bufferbloat*[7], causes that users experiment excessively long delays. And therefore, real-time services will not be available under such circumstances. Additionally, other important network performance parameters like link utilization and throughput are also very influenced by the buffer sizes, especially when TCP-alike protocols are used [13]. Based on the above, it becomes evident the necessity of dynamic buffer sizing mechanisms that cope with the performance degradation due to overbuffering. It also allows a better share of memory resources among different queues, which is valuable for multiple-interface/queues devices or resource-constrained devices.

Most of the buffer sizing schemes available in the literature [5][8] are adaptations of the well-known Bandwidth-Delay product (BDP) rule [2]. This rule states that the buffer size (B) must be at least $B = C \times RTT$ to achieve full link utilization. C represents the channel capacity and RTT is the average round-trip time of a TCP connection traversing that link. As it can be seen, these schemes are closely related to the congestion control mechanism of TCP. Nevertheless, since this research focuses on inelastic real-time services, UDP flows must be taken into account and alternative buffer sizing schemes are required. On the other hand, wireless devices impose additional challenges due to the fact that a node transmission state does not depend only on itself, but also on the state of the other nodes inside the same collision domain. These two facts have been taken into account in our previous work [1], where we presented a dynamic buffer sizing mechanism based on the maximum entropy principle. Section 3 presents a summary of this proposal.

The purpose of this work is to implement and evaluate the performance of the maximum entropy buffer sizing mechanism in wireless mesh networks (WMNs). WMNs are self-forming wireless multi-hop networks in which nodes may act as sources, destinations or forwarders of data packets. Important features like easy deployment and maintenance, self-configuration, robustness, etc. allow WMNs as potential alternative to provide a variety of applications and services in a diversity of fields. This work focuses on IEEE 802.11 based wireless mesh networks operating with QoS-enabled stations [13]. Different mesh scenarios have been considered to evaluate the impact of the number of hops and the routing modes over the buffer sizing mechanism.

The rest of this paper is organized as follows. Section 2 overviews the fundamentals of IEEE 802.11 enhancements to allow QoS and mesh networking, 802.11e and 802.11s respectively. The proposed mechanism to dynamically allocate the buffer size via maximum entropy is summarized in Section 3. Section 4 presents the evaluation of the algorithm in different wireless mesh network scenarios. Finally, Section 5 remarks the conclusions of this work.

2. AN OVERVIEW OF IEEE 802.11e AND IEEE 802.11s

2.1IEEE 802.11e

The default IEEE 802.11 Distributed Coordination Function (DCF) provides only best effort services. In this case, all traffic types compete in the same way for channel access. Intolerant real-time applications (e.g.: voice over IP, video conferences) requires to guarantee certain quality of services parameters like bandwidth, delay and delay jitter. To accomplish with these requirements the IEEE 802.11e group proposes the Enhanced Distributed Channel Access (EDCA) mechanism [13]. This mechanism improves and extends the original features of DCF and it is also the mandatory MAC scheme for Wireless Mesh Networks.

EDCA provides service differentiation and different priorities to four classes of services including: voice (*VO*), video (*VI*), best effort (*BE*) and background (*BK*). The different traffic classes are called Access Categories (ACs) and each of them has one specific priority queue (Fig. 1). Additionally in order to achieve priority differentiation, every AC has four important channel access parameters, which are: the minimum Contention Window (*CWmin*), the maximum Contention Window (*CWmax*), the Arbitration inter-frame space (*AIFS*) and the Transmission Opportunity (*TXOP*). *CWmin* and *CWmax* define the contention window range used for the backoff process. In the EDCA scheme, *CW* will be reset to *CWmin* immediately after a successful packet transmission. If there is a collision, *CW* will be doubled until reaches *CWmax*. The maximum allowed transmission time is defined by the *TXOP* limit: once a station accesses to the medium it can transmit one or more frames during *TXOP*. Finally, instead of using a fixed Distributed Inter Frame Space (*DIFS*), in EDCA an Arbitrary IFS (*AIFS*) is applied. The AIFS for a given AC is determined by the following equation:

$$AIFS[AC] = SIFS + AIFSN[AC] * aSlotTime \quad (1)$$

AIFSN is the AIFS number determined by the AC and the physical settings. The highest priority will be given to the AC with smallest AIFS. Table 1 shows the default parameters for the different ACs [13]:

Table 1. Standard EDCA Parameters

AC	CWmin	CWmax	AIFSN	TXOP Limit
AC_VO	3	7	2	1504us
AC_VI	7	15	2	3008us
AC_BE	15	1023	3	0
AC_BK	15	1023	7	0

As previously said, each AC has its own queue and it is possible that one or more classes tries to access to the medium at the same time, which is known as "internal contention". In this case, packets from highest priority queue (AC_VO) are served first due to their lowest backoff time.

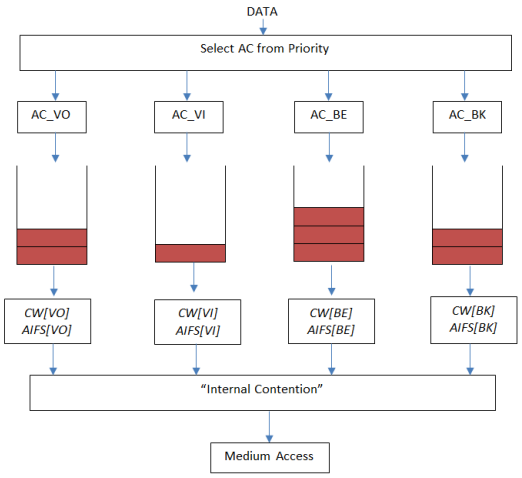

Figure 1. EDCA Queues

It is worth mentioning that EDCA MAC mechanism is not ideal technique for multi-hop networks since it has some problems such as: inefficient medium usage, unaware station problem, no transmission priorization of mesh STA over legacy STA [4]. However, these experiments have been evaluated using this mechanism as the mandatory standard for WMN and the unique one implemented in ns-3 simulator.

2.2 IEEE 802.11s

Wireless networks have been widely deployed in the last years. IEEE 802.11 standard for WLANs was mainly based in infrastructure mode and then some amendments have been proposed to improve bandwidth, coverage, security and Quality of Service. The demand of networks with higher capacity and coverage and at lower cost has motivated the emergence of infrastructure-less wireless networks. In this line, IEEE 802.11s Mesh Networking Amendment, now incorporated in the current IEEE 802.11-2012 standard [13], specifies MAC enhancements and new functionalities to support WLAN multi-hop mesh topologies.

Fig. 2 shows the typical WMN architecture. Here it is possible to identify four types of nodes: *Mesh stations* (mesh STA) which include mesh functionalities and participate in the creation and operation of the mesh cloud. They could be sources, destinations or forwarders of data traffic. *Mesh gates* allow the interconnection among different mesh basic service sets (MBSS) and with other infrastructure-based WLANs. The interconnection with any other external non-IEEE 802.11 network technology is possible through *Mesh Portals*. It is possible that gate, portal or access point (AP) functionalities are collocated in a single mesh device. Finally, traditional *non-mesh STAs* can access the mesh services through a mesh STA with gate and AP functionalities.

The main mesh functionalities required to establish and maintain a MBSS are summarized in the following.

The mesh discovery procedure can be carried out by a passive scanning of periodically sent Beacon frames or by an active scanning process using Probe Request/Response frames. These control frames must include the mesh identifier (Mesh ID) and the mesh profile information. The mesh profile specifies the attributes of a mesh network and contains the identifiers of: the mesh (Mesh ID), the path selection protocol, the path selection metric, the congestion control mode, the synchronization method and the authentication protocol. All the mesh STAs inside a MBSS must use the same mesh profile.

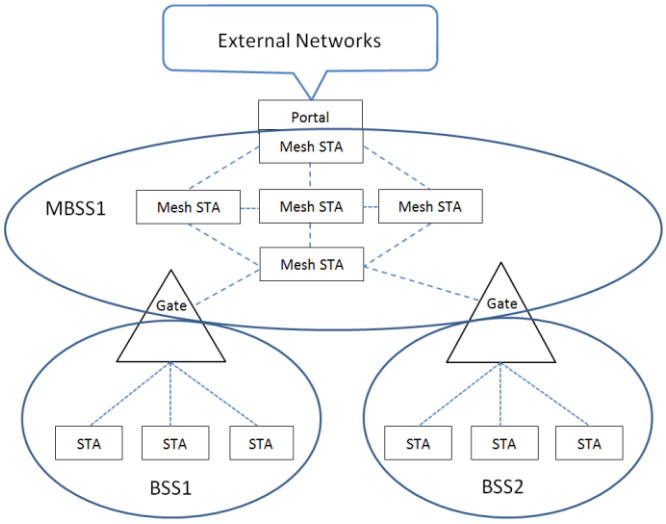

Figure 2. Typical architecture of the IEEE 802.11s WMN

After the discovery of a MBSS, and before data interchange, mesh stations must establish and maintain mesh peer links with their one-hop neighbors. This is done by means of the mesh peering management protocol. This protocol uses Mesh Peering Open, Mesh Peering Confirm, and Mesh Peering Close management frames to open, maintain and close links between neighbor mesh stations. All established peer links must be bidirectional. For this, a peer link is established only if both involved stations have sent Peering Open requests and have successfully received Peering Confirm responses. Although the standard does not specify when to close a peer link, the ns-3 network simulator peering management protocol implementation, used in this work, utilize a number of consecutive beacon loss or data transmission failures to detect peer link breakdowns [10][14].

For channel access, mesh STAs use the mesh coordination function (MCF). It consist of a contention-based channel access, specifically the EDCA mechanism described in the previous section, and an optional controlled channel access (MCCA) which is a reservation based channel access method. MCCA aims to optimize the efficiency of frame exchanges inside the mesh network by reducing the contention. This work only focuses on mesh STAs working with EDCA since it is the default and mandatory mechanism.

The key mesh functionality to provide layer-two multi-hop communications is the link layer routing or mesh path selection mechanism. The Hybrid Wireless Mesh Protocol (HWMP) is the mandatory and default path selection protocol. HWMP is an AODV-inspired [3] protocol that combines a reactive on-demand path selection with a proactive tree building mode. These two modes can be used concurrently. In the on-demand mode, when a mesh STA requires a path to another one, it broadcast a Path Request (PREQ) frame. When the request reaches its target, it responses with a unicast Path Replay (PREP) frame back to source mesh STA. In this way, mesh STAs communicate between them using peer-to-peer paths. In the proactive mode, at least one station must be configured as root mesh STA. The proactive tree to the root can be built in two different ways: using a proactive PREQ or by means of root announcement (RANN) frames, both of them are periodically sent by the root. The difference is that in the second case, path information to reach the root is distributed but there is no creation of forwarding paths. The ns-3 mesh model just implements the proactive PREQ mode and therefore, it is the only mode used in this work. The standard also allows that mesh stations may include alternative path selection protocols and metrics. Nevertheless, just one path selection protocol and metric shall be active at a given time.

The path selection protocol can use the default and mandatory airtime link metric to select the best path to a destination. The metric objective is to estimate the amount of channel resources required to transmit a frame over a specific link. This metric is computed according to the following equation [11]:

$$c_a = \left[O + \frac{B_t}{r} \right] \frac{1}{1 - e_f} \tag{2}$$

Where O is the channel access overhead, which depends on the PHY type and includes frame headers, training sequences, access protocol frames, etc. B_t is the test frame size (recommended 8192 bits). r is the date rate in Mbps at which mesh STA would transmit the test frame and e_f is the measured frame error rate for the test frame.

Standard also defines other mesh functionalities like security, power management, internetworking, intra-mesh congestion control, etc., but they are out of the scope of this work.

3. BUFFER SIZING VIA MAXIMUM ENTROPY

As it was previously mentioned, in this paper we present the implementation and the evaluation of the maximum entropy mechanism for Wireless Mesh Networks. The basic concepts of the mechanism and the extension to shared channels have been presented in our previous work [1]. To make this paper more self-contained, in the following a very brief summary of the mechanism is included.

The main goal of the buffer sizing mechanism is to allocate the minimum buffer size while satisfying a specific target packet loss probability. An analytical study of this loss probability in a system transmission (buffer and transmission channel) can be addressed by obtaining the state probabilities of a G/G/1/K queue at packet arrival time instants. Calling these probabilities a_i, $i=0,1,2,..,K$, the loss probability is a_K. However, the problem of obtaining those values is extremely complex, mainly because the need of knowing the probability density functions of the packet inter-arrival and packet service times. The complexity increases when it is needed to dynamically work over the time and therefore the probability functions continuously change. To avoid this difficulty, a maximum entropy approach is applied, but being compatible with two real measures: the channel utilization, ρ_a, and the average number of packets in the system N_a, both measured at the packet arrival times.

In the case we are analyzing, the value of a_0 is known:

$$a_0 = 1 - \rho_a \tag{3}$$

Therefore, the objective is to maximize the entropy of a_i:

$$\sum_{i=1}^{K} a_i \ln \frac{1}{a_i} \tag{4}$$

being compatible with the constraints provided by the real measures:

$$\sum_{i=1}^{K} a_i = \rho_a$$
$$\sum_{i=1}^{K} i \cdot a_i = N_a \tag{5}$$

The solution to this problem can be found in [1]. In this research not only G/G/1/K queue has been analyzed but also another system queues with different distribution functions, which demonstrates the correct behavior of the Dynamic Maximum Entropy (DME) mechanism. For our particular case, the loss probability P_L is given by:

$$P_L = a_K = \alpha \beta^K \tag{6}$$

where β can be obtained numerically from the expression [1]**¡Error! No se encuentra el origen de la referencia.**:

$$\frac{1}{1-\beta} \frac{1 - \left[(K+1) - K\beta \right] \beta^K}{1 - \beta^K} = \frac{N_a}{\rho_a} \tag{7}$$

and α is equal to [1]:

$$\alpha = \rho_a \frac{1-\beta}{\beta} \frac{1}{1-\beta^K} \tag{8}$$

Thus, to obtain the buffer size Q which satisfies a specific target packet loss probability P_L, we just need to isolate K in equation (6) and take into account that $Q=K-1$ in a one-server transmission system:

$$Q = \log_\beta \left(\frac{P_L}{\alpha} \right) - 1 \tag{9}$$

4. SIMULATION AND OBTAINED RESULTS

In this section, the behavior of the DME mechanism in WMN devices is presented. To do this evaluation, some simulations have been carried out over different scenarios in ns-3 simulator. Some ns-3 classes have been modified specially the one that manages EDCA queues. By default EDCA queues have a static queue size and with the DME mechanism implementation the queue sizes have to be adapted to the traffic load conditions in order to keep bounded the target packet loss probability. So, the DME mechanism manages the congestion of the network adapting the buffer sizes to the traffic load conditions, as long as the network is not overloaded or the buffer's capacity are not overflowed.

One important part of the DME implementation in ns-3, was done in `EdcaTxopN::Queue()` method of the class EdcaTxopN, since in this methodwasimplemented the previous equations 7 to 9. Next, it is presented a small ns-3 code part of this class:

```
Q=m_queue->GetMaxSize();
prevQ=Q;
uint32_t N=Q+1;
betaa_max = 10.0;
betaa_min = 0.0;

do {
betaa = (betaa_max + betaa_min) / 2;
     y = ((1.0 + (N * betaa - N - 1) *
          pow(betaa, N)) /((1 - betaa) *
          (1 - pow(betaa, N))))-(m_averagedNa /
        m_averagedRhoa);
if (y > 0) {
betaa_max = betaa;
     } else if (y < 0) {
betaa_min = betaa;
     }

} while ( abs(betaa_max-betaa_min) > 0.00001);

alfaa = (m_averagedRhoa * (1 - betaa)) /
(betaa * (1 - pow(betaa, N)));
newN = (1 / log10(betaa)) * log10(m_pL / alfaa);
if (newN<1) {
    Q=1;
} else {
  Q = floor(newN);
  }
}

if (Q >m_queue->GetSize()) {
neededQ=Q;
} else {
neededQ=m_queue->GetSize();
}
dif=neededQ-prevQ;
```

In the following subsections, the obtained results are presented in two evaluated WMN scenarios.

4.1 First scenario: mesh chain topology

The first considered scenario is shown in Fig. 3. This scenario is a mesh chain topology, although it does not represent a common real situation, it was considered to observe what are the appropriate parameters to operate the network in stable conditions and how the number of hops (*H*) affects the WMN performance. First of all, to find out the load traffic conditions and the appropriate WMN parameters to obtain peer-links stability some experiments were carried out with a static buffer size. These obtained parameters are used in the rest of simulations and therefore they are provided in the corresponding tables.

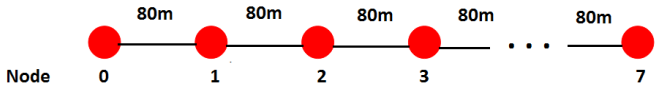

Figure 3. Scenario-1: mesh chain topology

For the second set of experiments the dynamic buffer sizing mechanism is enabled. In this scenario, the main objectives of the experiments are: to test the correct behavior of the DME mechanism when it is used in the set of queues specified by IEEE 802.11e and to observe in this situation the effect of the number of hops (*H)* in the network performance.

To drive the simulations, a variable packet rate is generated in the traffic source. Therefore, the buffer size must be adapted by the DME mechanism over time due to this variable rate. The considered traffic pattern is shown in Fig. 4. Some other relevant parameters used in these simulations are presented in Table 2.

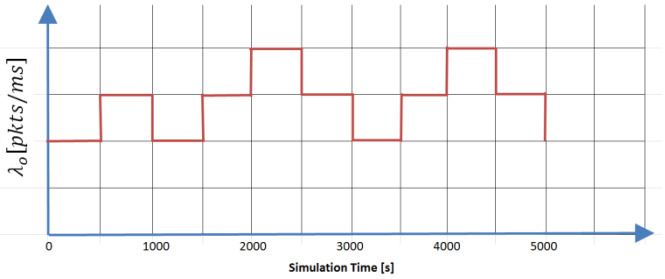

Figure 4. Traffic pattern (packets/ms)

Table 2. Simulation parameters for the Scenario-1

SIMULATION DATA	
Mean Packet Length (Truncated Exponential Distribution)	200B
Mean packet arrival rate (Exponential Distribution)	Flow 1: 1paq/5ms Flow 2: 1paq/6ms Flow 3: 1paq/7ms
Mean Tx bit rate	Flow 1: 320kbps Flow 2: 266kbps Flow 3: 228kbps
Qinit	100
Simulation Time	5000 s
RTS/CTS	Off
EDCA ACs	AC_BE and AC_VO
HWMP mode	Reactive
Path Discovery Mechanism	ON once in all simulation
MaxBeaconLoss	5
MaxPacket-Failure	5

The analysis of the DME implementation in WMN nodes have been done in the similar way than in the other previous researches [1]. The interesting parameters to observe are: the average channel utilization (ρ_a), the queue size, the Packet Loss Ratio (PLR) and the delay. So, the following figures show the results of the application or implementation of the DME mechanism in the WMN. The influence of the number

of hops (*H*) between source and destination can be seen in Fig. 5, where the average channel utilization over time is presented (for the service class AC_BE and a requested loss probability P_L=10^{-3}). It can be seen that the average channel utilization increases with *H* due to the transmissions of the intermediate nodes. As a direct consequence, also the needed buffer size grows with *H* in order to keep bounded the target P_L, as it is depicted in Fig. 6. The same results for another service class, AC_VO, are presented in Figs. 7 and 8.

In order to check the correct behavior of the implemented DME algorithm we present a set of figures with relevant parameters. For example, fig. 9 shows the packet loss ratio in the node 0 for the two service classes previously analyzed.

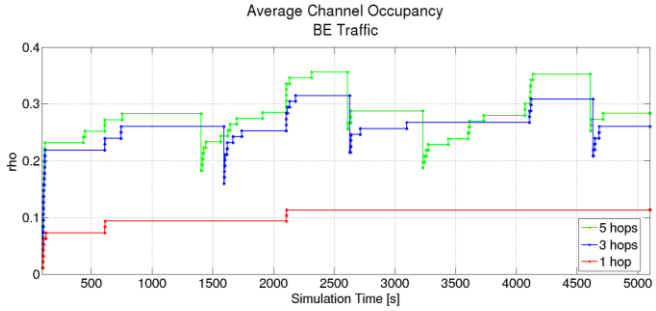

Figure 5. Average channel utilization vs. number of hops for AC_BE

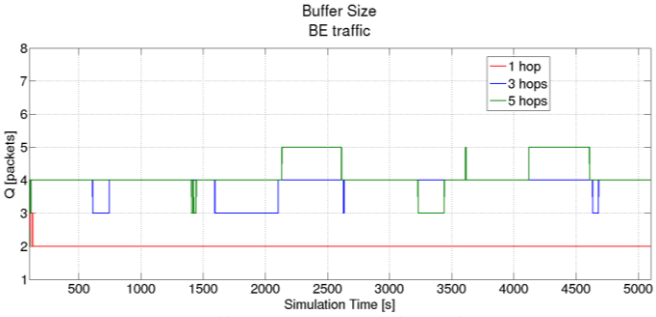

Figure 6. Buffer size vs number of hops for AC_BE

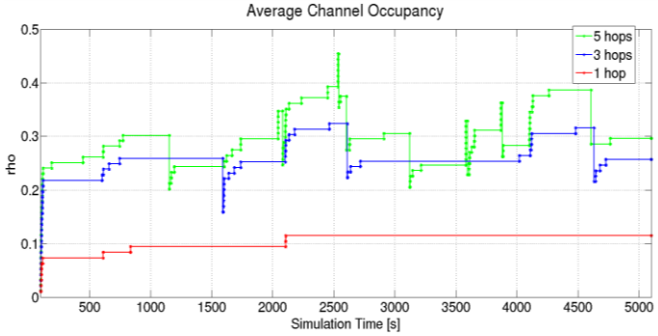

Figure 7. Average channel utilization vs. number of hops for AC_VO

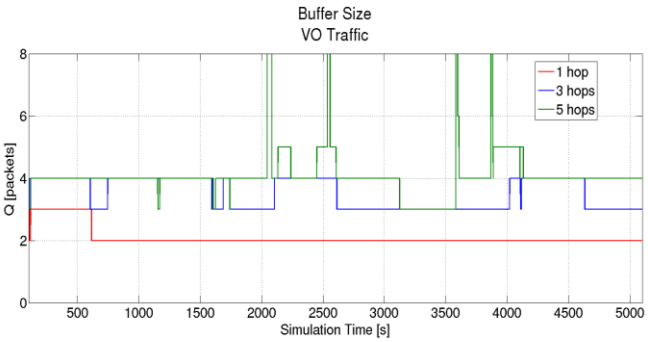

Figure 8. Buffer Size vs. number of hops for AC_VO

In the previous results, two target loss probability values have been considered: 10^{-3} and 10^{-4}. These values, in real applications, depend on the traffic type, for example for voice acceptable losses are lower than 1%. For higher demand applications lower values such as 10^{-3}, 10^{-4} , 10^{-5} , etc. can be necessary to guarantee; that is why this research and the previous ones, for the WLANs[1] and for the dedicated networks, take these values as references. These simulations show that in WMN it is important to consider the network size in the network dimensioning because from certain number of hops (5 or 6 in the figure) the target P_L is not achieved (in these cases, the channel utilization grows abruptly due to the transmissions of the intermediate nodes and what is the same, the network is overloaded). However, when the network is not congested, the implemented mechanism works correctly and offers the desired quality of service in terms of buffer overflows. All of these previous statements regarding to the number of hops in WMN, verify the recommended values from some vendors in real WMN deployments cases, where it is said that the performance of the network is inverse of the number of hops (*1/H*) and therefore no more of 3 or 4 hops are recommended from one mesh station to the gateway [6]0.

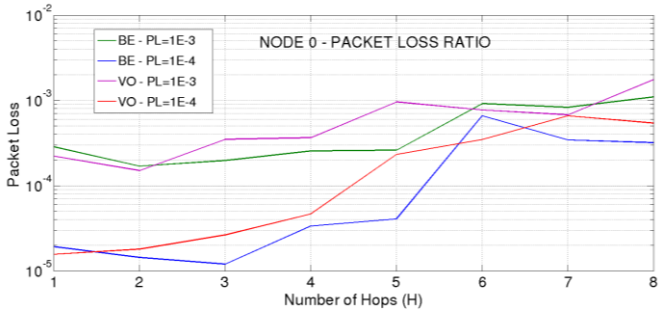

Figure 9. Packet loss ratio vs. number of hops

The last experiments carried out in this scenario are related to the packet service and transfer times. First, Fig. 10 shows the service time p.d.f. for the AC_VO traffic class and *H*=4. It must be taken into account that we consider the service time in its classical definition, that is, the time elapsed between the beginning of a packet transmission until the beginning of the transmission of the next packet in the queue. In other words, the service time includes all the needed retransmissions until a packet is successfully received, and therefore the device can start the transmission of the next packetwaiting in the queue.

In this experiment, the number or retransmissions is very low, and so the service time is very similar to the transmission time. As the distribution of the packet length is exponential (see Table 2), the service time p.d.f. in Fig. 10, fits also very accurately to the exponential distribution function. In general terms the net devices in this experiment can be modelled as M/M/1 queue.

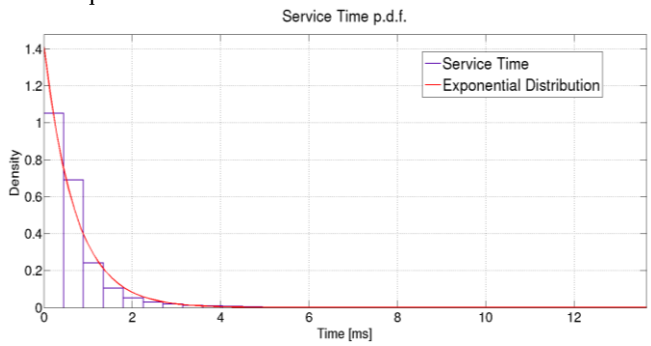

Figure 10. Service Time pdf for 1x5 Mesh Topology and VO traffic

To observe the impact in the service time when more retransmissions occur in the network, a new set of simulations was carried out including variable losses in the transmission channel. This way, more than one attempt of transmission per packet was necessary. Fig. 11 shows the service time pdf for the same traffic and topology but with a higher number of transmission attempts (3.3406 in average) per packet. As it can be seen, in this case the p.d.f. is best fitted with a Gamma distribution.

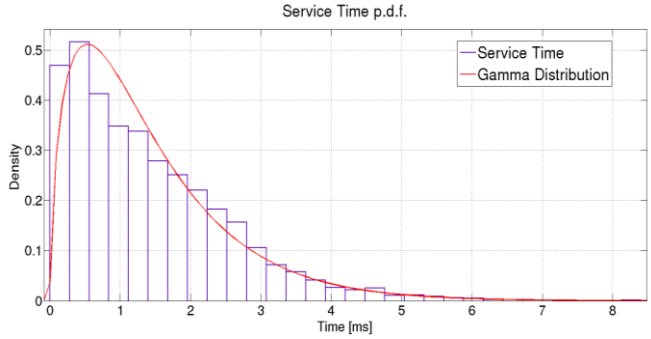

Figure11. Service Time pdf for 1x5 Mesh Topology and VO traffic

Finally, the end-to-end or transfer time is analyzed. As we are working with very low packet loss probabilities, this time is very similar for all of them. This fact can be checked in Table 3, where the transfer time (wait plus service) in every node and the end-to-end time are presented for two targetP_L (10^{-3} and 10^{-4}). It is important to mention that these obtained time delays are for the scheduler provided by EDCA mechanism. In addition to this, these times varies for different access categories especially when the number of hops grows, as it can be seen in Fig. 12. For a few number of hops (e.g. lower than 3 hops), the end-to-end delay is not so much different between traffic classes, but from 4 hops and forwards the delay is increasingly lower for access category AC_VO than for AC_BE.

Table 3. Mean transfer time T and end-to-end time $T_{EE}$for 1x7 mesh chain topology

AC= VO		**Target P_L 10^{-3}**	**Target P_L 10^{-4}**
Topology	**Node**	**T_i[ms]**	**T_i[ms]**
1x7 N0 → N6 6 Hops	N0	0.93152	0.93056
	N1	0.86983	0.87775
	N2	0.82855	0.83414
	N3	0.64975	0.64859
	N4	0.59868	0.59868
	N5	0.5854	0.58467
$T_{EE}[ms]$		4.4637	4.4744

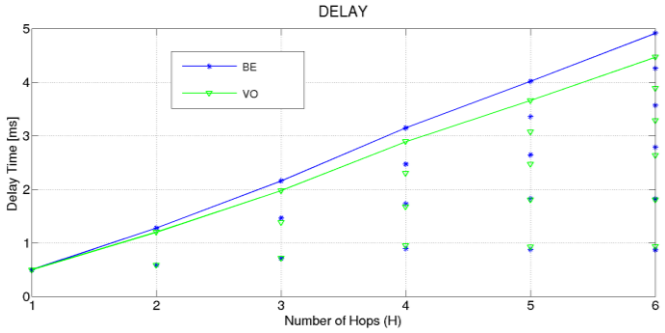

Figure 12. Delay vs. number of hops

4.2 Second scenario: mesh star topology

The second scenario and the parameter values used in the simulations are shown in Fig. 13 and Table 4 respectively. The values shown in the Table 4 are the appropriate reference values; the packet length has an exponential distribution function from 64B to 1500B with mean packet length of 200B according to the internet common traffic. The mean transmission rate is also a common rate for wireless internet users. The simulation time (5000s) is a considerable period to evaluate the operation of the algorithm. RTS/CTS mechanism has been deactivated according to recommendations of researches, since RTS/CTS mechanism produces a negative impact in WMN performance, the Conservative Energy Detection (ED) and Physical-Carrier Sense (P-CS) threshold settings prevents almost any occurrences of hidden station problem in 802.11, and it only adds overhead [4]. The rest of the simulation parameters represent the given and default recommended values in ns-3 WMN implementation [10][14]. On the other hand, the scenario consists on a central node (N4 in the figure, which can act as a Portal Mesh STA node or a Gate) communicating with different peripheral mesh STA nodes (N0, N2, N6 and N8). This scenario although may be considered a short part of real WMN deployment, it represents a subsection interesting to analyze, especially because the shared wireless medium is used every time in the simulation period, as it is depicted in the Fig. 14. Here, we can see the gateway simultaneous transmissions to peripheral

mesh STA nodes represented with the numbers: 0, 2, 6 and 8 and the intermediate nodes are: N1, N3, N5, N7, which forward the information. Therefore, the multiple traffic sources occur due to retransmission of these intermediate mesh nodes. Moreover, real WMN deployment cases recommend 8 to 15 mesh stations by one gateway [6]0. Finally, this situation can be considered as a stress environment, since the traffic load conditions are higher than the real carried traffic in a network, or what is the same the medium access contention is higher than in a real situation considering the statistical multiplexing.

In addition to this, the nodes are distributed in different positions and distances between them in order to not overlap coverage areas. In the Fig. 13, the peer-links (highlighted in blue) established between mesh STA nodes are also depicted. Under normal conditions, when all links are up, the Gate node communicates with the peripheral STA mesh nodes in two hops, according to the HWMP path selection mechanism. It transmits alternatively to the peripheral mesh nodes through the intermediate nodes. Therefore, the channel load fluctuation is not only due to the traffic generated by central node but also due to the activation/deactivation (ON/OFF) of the other stations that share the medium.

Other time, as in the previous scenario-1 the interesting parameters to observe are: the average channel utilization (ρ_a), the queue size and the delay. The channel load fluctuation seen by the Gate node, it is shown in Fig. 15 for two access categories. Consequently, the allocated buffer size must follow that fluctuation, as it is shown in Figs. 16 and 17 for the same two access categories and for two different target P_L values.

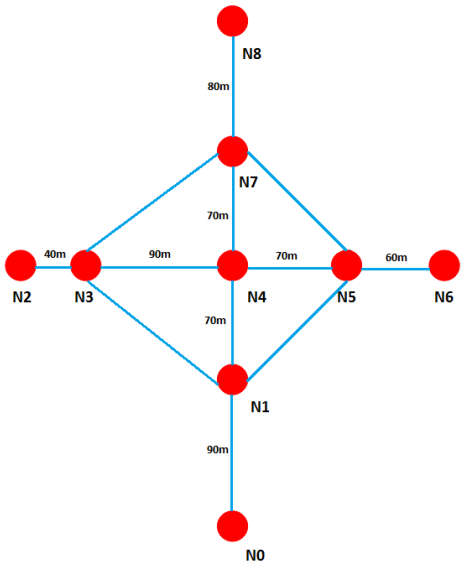

Figure 13.Mesh network topology for scenario-2.

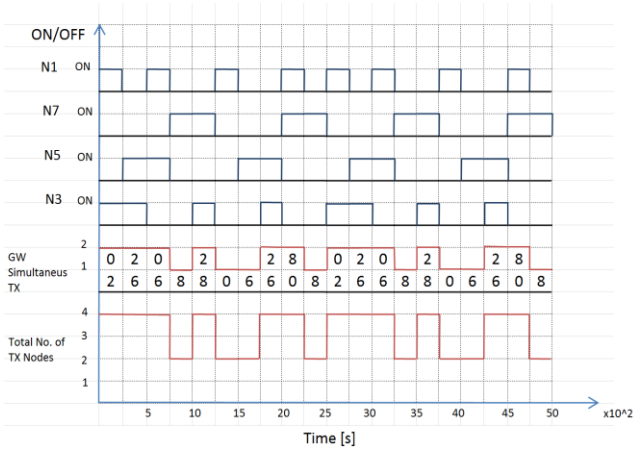

Figure 14.Offered Load or traffic pattern in scenario-2.

To measure one of the advantages obtained with theapplication of the DME mechanism, the concept of memory utilization efficiency is used. This efficiency is defined as the ratio between the area under the buffer occupancy curve and the area under the buffer size curve [1]. These two curves are shown for one of our experiments (best-effort category and P_L=10^{-3}) in Fig. 18. Table 5 presents the comparison of the memory utilization efficiency (η) between static and dynamic buffer size allocation. To do a consistent comparison, the buffer size selected with the static allocation must be the one that produces the same loss probability than the dynamic allocation. To obtain these sizes, it is necessary to carry out a previous set of simulations until the desired P_L is achieved. Observe that in the practice this is not possible, which represents another advantage of the proposed DME mechanism. Besides, with this scenario and simulations, the results show that the improvement achieved in the memory utilization efficiency with the dynamic mechanism is higher than 9% for AC_BE and AC_VO.

Table 4. Simulation parameters for the scenario-2

SIMULATION DATA	
Flows	Flow 1: N4 → N0 Flow 2: N4 → N2 Flow 3: N4 → N6 Flow 4: N4 → N8
Mean Packet Length (Exp. Distribution)	200 B
Mean packet arrival rate (Exp. Distribution)	1paq/6ms
Mean Tx bit rate	267 kbps
Qinit	100
Simulation Time	5000 s
RTS/CTS	Off
EDCA ACs	AC_BE and AC_VO
HWMP mode	Reactive&Proactive
Path Discovery Mechanism	ON each 5.12 s (default ns-3 value)
MaxBeaconLoss	5
MaxPacket-Failure	5
Confident interval of the results	95%

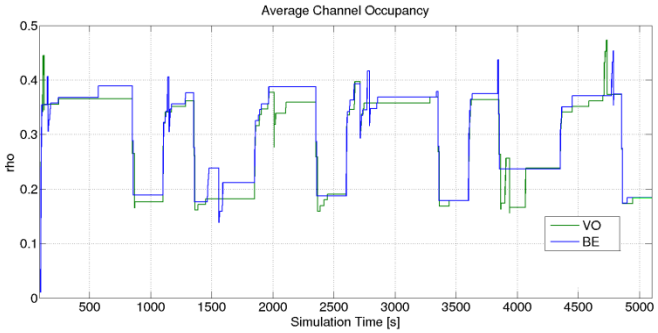

Figure 15.Average channel utilization for AC_BE and AC_VO and target P_L=1E-3

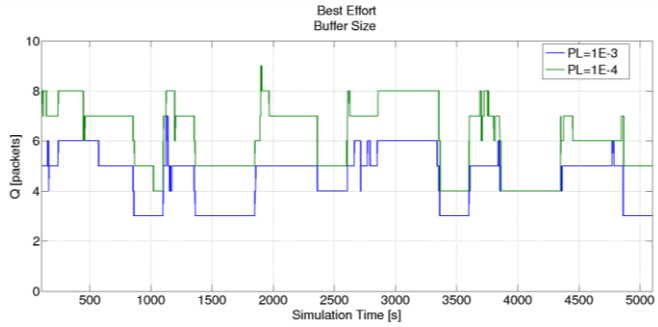

Figure 16. Buffer size in for different values of the target P_L and AC_BE

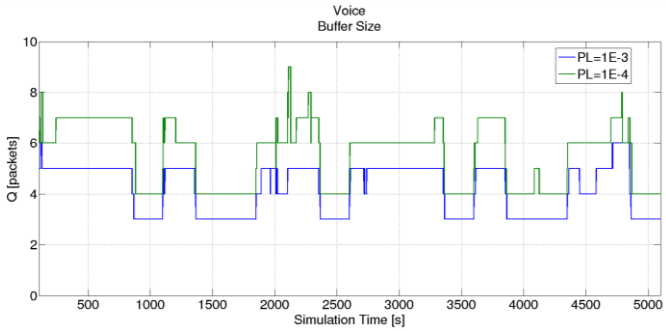

Figure 17. Buffer size for different values of target P_L and AC_VO

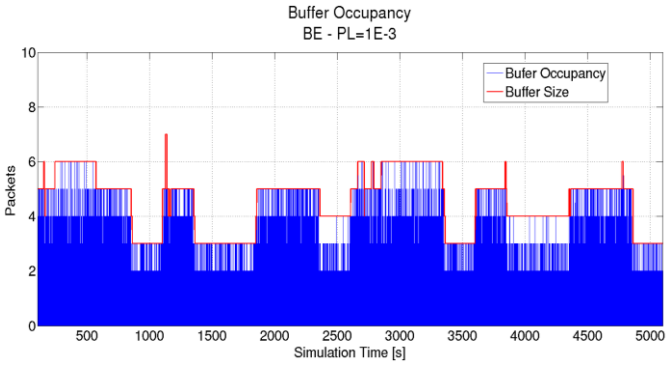

Figure 18. Buffer size vs. buffer occupancy

Table 5. Memory efficiency comparison between static and dynamic buffer size for for two ACs

AC	*Q* for static [pkts]	η_static_Q	η_dynamic_Q	% Improvement
BE	$P_L = 10^{-3}$	0.01655	0.01829	10.51%
	5			
	$P_L = 10^{-4}$	0.01188	0.01364	14.81%
	7			
VO	$P_L = 10^{-3}$	0.01499	0.01699	13.34%
	5			
	$P_L = 10^{-4}$	0.01193	0.01298	8.80%
	6			

On the other hand, regarding to the delay analysis different times were obtained with static and dynamic buffer sizes in order to compare the results between them. The wait, service and transfer packet times are presented in tables 6 and 7 for best effort and voice access categories respectively, where we can see that those different delays are practically independent of the mechanism (dynamic or static) used.

Table 6. Mean wait, service and transfer time for AC_BE and target P_L=10^{-3}

	Dynamic_*Q*			Static *Q*=5		
Node	T_w [ms]	T_s [ms]	T [ms]	T_w [ms]	T_s [ms]	T [ms]
4	0.3726	0.4843	0.8569	0.4078	0.4888	0.8965
1	0.3189	0.4807	0.7996	0.3296	0.4844	0.8139
3	0.3066	0.4708	0.7775	0.3360	0.4849	0.8209
5	0.3181	0.4786	0.7967	0.3248	0.4790	0.8038
7	0.2488	0.4716	0.7204	0.2482	0.4702	0.7185

Table 7. Mean wait, service and transfer time for AC_VO and target P_L=10^{-3}

	Dynamic *Q*			Static *Q*=5		
Node	T_w [ms]	T_s [ms]	T [ms]	T_w [ms]	T_s [ms]	T [ms]
4	0.3308	0.5291	0.8599	0.3282	0.5288	0.8570
1	0.1908	0.5017	0.6926	0.1886	0.5023	0.6910
3	0.1921	0.4821	0.6742	0.1913	0.4825	0.6738
5	0.1943	0.4977	0.6920	0.1976	0.4988	0.6964
7	0.1476	0.4784	0.6260	0.1490	0.4790	0.6280

In the previous experiments, the reactive HWMP was used. In comparison to the proactive HWMP mode, the results are no so much different. However, focusing on the loss probability, it can be observed that, for the most stringent considered value (10^{-4}), the obtained result for the reactive mode is slightly higher than the one obtained for the proactive mode. Table 8 presents the values for the Gate node.

Table 8. Packet Loss for AC_BE and two HWMP modes in node GW

	Reactive HWMP mode		Proactive HWMP mode	
Node	Target P_L 10^{-3}	Target P_L 10^{-4}	Target P_L 10^{-3}	Target P_L 10^{-4}
Gate	$4.18 \cdot 10^{-4}$	$1.73 \cdot 10^{-4}$	$2.16 \cdot 10^{-4}$	$2.33 \cdot 10^{-5}$

5. CONCLUSIONS

In this paper, the problem of dynamically allocate the buffer size in wireless mesh network devices has been addressed. To this end, a dynamic buffer sizing mechanism based on the maximum entropy principle has been simulated, analyzed and evaluated in several WMN scenarios. This Dynamic Maximum Entropy (DME) mechanism has been previously tested over classical WLANs, showing a very good behavior.
However, WMN present two characteristics that must been taking into account. First, they use the mandatory MAC mechanism IEEE 802.11e standard with four different access categories, which means the presence of four different buffers, with the advantage that the DME can manage them independently, each one with different requirements of packet loss probabilities. Second, they are multi-hop wireless networks, and therefore the same packet can be retransmitted by more than one device over the shared medium.
To evaluate the mechanism, thisone has been implemented and incorporated to the mesh module in the ns-3 simulator. In order to extract results and conclusions, two different simulation scenarios have been taken into account. The first and main conclusion is that the DME mechanism works also in a correct way on WMN devices, that is, it provides the minimum buffer size that keeps the loss probability under a previously selected value. The WMN devices are able to self-configure their buffer sizes, and they capture the network load fluctuations (which can be caused not only for their own traffic variation, but also for the activation/deactivation of other devices that share the transmission medium) and dynamically adapt the buffer size.
Another important conclusion is that the needed buffer size to guarantee a maximum loss probability increases with the network size (in terms of number of hops). This is due to the increment in the shared channel utilization caused by the packet retransmissions of the intermediate nodes. So, it is important to consider the number of hops from one mesh node to the gateway in the network dimensioning. Typical recommended values are 3 to 4 hops.
The advantage of DME versus static allocation in terms of memory optimization has also been proved. This provides a benefit in network devices with multiple interfaces as well as in resource-constrained devices. Finally, the time delay analysis shows that the transfer time (wait plus service time) is independent from mechanism (static or dynamic buffer sizing) used; moreover, as the target packet loss probabilities are very low, the transfer time is also independent from them.

Further work is on-going to apply the DME mechanism to the design of all-optical routers where small buffers are much appreciated. In this scenario, the utilization of different schedulers is also taken into account. This way, different QoS could be provided to different flows, not only in terms of loss probability but also in terms of waiting time. Other future lines of work are the evaluation of the algorithm for TCP and a mix of TCP and UDP flows, and the implementation and evaluation of the dynamic mechanism in other network simulators. Moreover, as it was mentioning, the DME mechanism via maximum entropy uses a target P_L to dynamically adapt the buffer size to the network load. If some other variable is introduced such as counters of aging algorithms the requested packet loss probability can be affected positively. For this, the EDCA queues have to be modified.

REFERENCES

[1] A. Vázquez-Rodas, L.J. de la Cruz Llopis, M. Aguilar Igartua and E. Sanvicente Gargallo, “Dynamic buffer sizing for wireless devices via maximum entropy”, Comput. Commun. (2014), http://dx.doi.org/10.1016/j.comcom.2014.03.003.

[2] C. Villamizar, C.Song, “High performance TCP in ANSNET”, SIGCOMM Comput. Commun. Rev. 24, 5 (1994), pp. 45-60.

[3] C. Perkins , E. Belding-Royer , S. Das, “Ad hoc On-Demand Distance Vector (AODV) Routing”, RFC 3561, 2003.

[4] G. Hiertz, S. Max, R. Zhao, D. Denteneer, and L. Berlemann, “Principles of IEEE 802.11s” in Proc. ICCCN, Aug. 2007, pp. 1002–1007.

[5] G. Appenzeller, I. Keslassy, and N. McKeown, “Sizing router buffers”, SIGCOMM Comput. Commun. Rev. 34, 4 (2004), pp. 281-292.

[6] Huawei Techonologies Co, Ltd, “Mesh Technology White Paper”, Mayo 2013.

[7] J. Gettys and K. Nichols, “Bufferbloat Dark Buffers in the internet”, Communications of the ACM, vol 55, n. 1, 2012, pp. 57-65.

[8] K. Jamshaid, B. Shihada, L. Xia, P. Levis, “Buffer Sizing in 802.11 Wireless Mesh Networks”, Mobile Adhoc and Sensor Systems (MASS), 2011 IEEE 8th International Conference on, (2011), pp. 272-281.

[9] K. Chei, Y. Xue, S.H. Shah, and K. Nahrstedt, “Understanding bandwidth-delay product in mobile ad hoc networks”, Computer Communications, 27 (2004), pp. 923-934.

[10] Kirill Andreev, Pabel Boyko, “IEEE 802.11s Mesh Networking NS-3 Model”, workshop on ns-3, 2010, unpublished. Available: http://www.nsnam.org/workshops/wns3-2010/dot11s.pdf.

[11] L. L. H. Andrew, T. Cui, J. Sun, M. Zukerman, K.-T. Ko and S. Chan, “Buffer sizing for nonhomogeneous TCP sources”, IEEE Communications Letters, vol. 9, no. 6, pp. 567- 569, June 2005.

[12] T. Li, D. Leith and D. Malone, “Buffer Sizing for 802.11-Based Networks”, IEEE/ACM Transactions on Networking, vol.19, no.1, (2011), pp. 156-169.

[13] IEEE Wireless LAN Medium Access Control (MAC) and Physical Layer (PHY) Specifications, IEEE 802.11-2012 standard, February 2012.

[14] ns-3 network simulator, available online at: http://www.nsnam.org

Sendar Vural, Dali Wei, and Klaus Moessner, “Survey of Experimental Evaluation Studies for Wireless Mesh Networks Deplyments in Urban Areas Towards Ubiquitous Internet”, IEEE Communications Surveys & Tutorials, Vol. 15, No. 1, 2013, pp. 223-239.